

1 Total Organic Carbon in the Bowland- 2 Hodder Unit of the southern Widmerpool 3 Gulf: a discussion.

4 Jan A. I. Hennissen*

5 Christopher M. A. Gent

6 British Geological Survey, Environmental Science Centre, Keyworth, Nottingham, NG12 5GG,
7 United Kingdom

8 *Corresponding author: janh@bgs.ac.uk

9 Abstract

10 This review of the article by Kenomore et al. (2017) on the total organic carbon (TOC) evaluation of
11 the Bowland Shale Formation in the Widmerpool Gulf sub-basin (southern Pennine Basin, UK)
12 reveals a number of flaws, rooted mostly in an inadequate appreciation of the local mid-Carboniferous
13 stratigraphy. Kenomore et al. use the $\Delta\text{Log R}$, the ‘Passey’ method after Passey et al. (1990), to
14 evaluate the TOC content in two boreholes in the Widmerpool Gulf: Rempstone 1 and Old Dalby 1.
15 We show here that Kenomore and co-authors used maturity data, published by Andrews (2013), from
16 different formations to calibrate their TOC models of the Bowland Shale Formation (Late
17 Mississippian–Early Pennsylvanian); the Morridge Formation in Rempstone 1 and the Widmerpool
18 Formation in Old Dalby 1. We contest that this gives viable TOC estimates for the Bowland Shale
19 Formation and that because of the location of the boreholes these TOC models are not representative
20 over the whole of the Widmerpool Gulf. The pyrite content of the mudstones in the Widmerpool Gulf
21 also surpasses the threshold where it becomes an influence on geophysical well logs. Aside from these
22 stratigraphic and lithologic issues, some methodological flaws were not adequately resolved by
23 Kenomore and co-authors. No lithological information is available for the Rock-Eval samples used
24 for the maturity calibration, which because of the interbedded nature of the source formations, has
25 implications for the modelling exercise. We recommend that more geochemical data from a larger
26 array of boreholes covering a wider area, proximal and distal, of the basin are collected before any
27 inferences on TOC are made. This is necessary in the complex Bowland Shale system where
28 lithological changes occur on a centimetre scale and correlations between the different sub basins are
29 not well understood.

30 1. Introduction

31 The Pennine Basin is a Carboniferous depocentre that underlies most of northern England and
32 consists of a patchwork of fault-bounded basins separated from each other by carbonate blocks
33 (Figure 1a). In recent years, the Pennine Basin has received renewed attention from the research and
34 industrial community because some of its successions, in particular the Bowland Shale Formation and
35 its lateral equivalents (e.g. the Morridge Formation), were identified as potentially prospective targets
36 for shale gas and oil (Selley, 1987; Smith et al., 2010). One of the sub-basins, the Widmerpool Gulf,
37 is the subject of a recent study by Kenomore et al. (2017) with the remit of:

38 ‘evaluating the total organic carbon (TOC), for the Bowland Shale Formation in the Upper Bowland
39 using conventional well logs (sonic and resistivity logs) from two wells namely, Rempstone 1 and Old
40 Dalby 1 using Passey's $\Delta\text{Log R}$ method proposed by Passey et al. (1990)’ (Kenomore et al. 2017,
41 p.137).

42 There is a relative paucity of organic geochemical (including TOC) data for the Bowland Shale in the
43 public domain. For example, the Andrews (2013) report for the Pennine Basin in its entirety only
44 contains 109 Rock-Eval pyrolysis data points (17 boreholes; 1028.25m of core). Kenomore et al.
45 (2017) had potential to be a valuable addition to the sparse dataset characterizing this potentially
46 important source of indigenous energy in the UK. However, a detailed analysis of the paper revealed
47 many misconceptions and shortcomings. Taken together, these observations ultimately result in the
48 misleading conclusion that:

49 ‘Passey’s method is a suitable method to estimate TOC as the value bears a close resemblance to
50 estimates obtained from British Geological Survey (BGS) Rock-Eval core analysis report (*sic*).’
51 (Kenomore et al., 2017, p.143).

52 We believe these shortcomings stem from an incomplete understanding of the complex local
53 stratigraphy in the Widmerpool Gulf combined with an oversimplified representation of the $\Delta\text{Log R}$
54 method to assess TOC in the Bowland Shale Formation. These are the main reasons for the
55 conception of the current manuscript. As pointed out, but inadequately referenced, on p. 138 in
56 Kenomore et al. (2017), the $\Delta\text{Log R}$ method (colloquially called the ‘Passey technique’, following
57 Passey, 1990) was used before to assess TOC values of Jurassic shales of the Weald Basin (Gent et
58 al., 2014 in Andrews, 2014) but was hitherto not applied to the Carboniferous data set from the
59 Pennine Basin.

60 To eradicate some of the misconceptions, we present below the necessary stratigraphic background in
61 the Widmerpool Gulf (Section 2), the assumptions inherent to and limitations of the $\Delta\text{Log R}$ (Passey)
62 method when applied to the Carboniferous Widmerpool Gulf succession (Section 3), a reinterpretation
63 of the well logs using the $\Delta\text{Log R}$ method of Rempstone 1 and Old Dalby 1 with a short discussion

64 highlighting the aforementioned uncertainty (Section 4), followed by concluding remarks and
65 suggestions for future research (Section 5).

66 2. Stratigraphic and palaeogeographic notes

67 In the context of studying the organic rich Carboniferous mudstones identified as the most prospective
68 intervals for unconventional hydrocarbons (Selley, 1987; Smith et al., 2010), it is necessary to review
69 the local stratigraphy of the Pennine Basin. The Widmerpool Gulf is the southernmost sub-basin of
70 the Pennine Basin, and is one of many fault-bounded sub-basins that formed during the Chadian–early
71 Arundian and late Asbian–Brigantian rift-driven fragmentation of Early Palaeozoic deposits (Fraser et
72 al., 1990; Gawthorpe, 1987). Under the influence of the thermal sag phase of basin development, an
73 epi-continental sea transgressed the Pennine Basin with the Southern Uplands and Wales-Brabant
74 High still emerging (Figure 1) (Leeder, 1982; Leeder and McMahon, 1988). During the course of the
75 Namurian (Serpukhovian–Bashkirian), these basins were filled in with deltaic successions originating
76 from the emerging land masses. However, the deltaic deposits are interspersed by intervals rich in
77 ammonoid and bivalve fauna that have been termed ‘marine bands’ (Bisat, 1923). These depositional
78 intervals representing maximum flooding surfaces (Gross et al., 2014) with an estimated periodicity of
79 111 kyr (for the Pendleian–Arnsbergian) (Waters and Condon, 2012) reflecting glacio-eustatic sea
80 level fluctuations (Isbell et al., 2003; Stephenson et al., 2008; Veevers and Powell, 1987). In the
81 Namurian as a whole, 60 marine bands with an average duration of 180 kyr, have been recognized
82 (Martinsen et al., 1995) of which 46 correspond to the occurrence of a key goniatite species (Bisat,
83 1923; Holdsworth and Collinson, 1988; Ramsbottom, 1977; Ramsbottom et al., 1962).

84 2.1 Carboniferous deposits in the Widmerpool Gulf

85 The Carboniferous stratigraphy of the Widmerpool Gulf, summarized in Figure 2, reflects the
86 palaeogeographic changes the area underwent: a fault-bounded rift topography created during the Late
87 Devonian was gradually infilled during the Visean, punctuated with transgressions in the Namurian
88 and evolved to a richly forested fluvial plain giving rise to extensive coal horizons by the
89 Pennsylvanian (Aitkenhead et al., 2002). A complete overview of all the Carboniferous deposits
90 proven in the Widmerpool Gulf are given by Waters et al. (2007) and Waters et al. (2009). For the
91 purposes of this manuscript it suffices to highlight the composition and palaeogeography of the
92 Widmerpool, Bowland Shale and Morridge Formations and the Millstone Grit Group.

93 The Widmerpool Formation, formally defined by Aitkenhead and Chisholm (1982), consists of dark
94 to pale brown, calcareous or carbonaceous, locally pyritic, fissile mudstones, interbedded with
95 turbidites consisting of quartzose/calcareous siltstone and sandstones (Waters et al., 2009). This
96 formation is a predominantly turbiditic deposit with southerly-sourced sediments mainly derived from
97 the Wales-Brabant High (Aitkenhead et al., 2002)

98 The upper part of the Craven Group is represented by the Bowland Shale Formation (in this area,
99 formerly termed the ‘Edale Shales’, Waters et al., 2007), which has a highly diachronous upper
100 boundary across the sub-basins of the Pennine Basin: early Pendleian in the Craven Basin (Riley,
101 1990); Kinderscoutian in the Widmerpool Gulf (Figure 2; Waters et al., 2007) and Yeadonian in
102 North Wales (Davies et al., 2004; Waters et al., 2007). In the Widmerpool Gulf, the Bowland Shale
103 Formation passes laterally southwards into the sandstone dominated Morridge Formation (Millstone
104 Grit Group) which accumulated along the northern margin of the Wales-Brabant High (Waters et al.,
105 2009).

106 The Morridge Formation was introduced as a distinct unit by Waters et al. (2009) to highlight the
107 different source area for the fluvio-deltaic successions from the rest of the Millstone Grit Group found
108 in the more northern parts of the Pennine Basin. The Morridge Formation contains pale
109 protoquartzitic sandstone intervals sourced from the Wales Brabant High while the terrestrial material
110 for the remainder of the Millstone Grit Group is sourced from the north. Lithologically, the Morridge
111 Formation consists of interbedded dark grey, shaly mudstones and pale protoquartzitic silt- to
112 sandstones interpreted as turbiditic sand bodies and shallow-water fluvio-deltaic facies (Waters et al.,
113 2009).

114 2.2 The Bowland-Hodder Unit

115 Andrews (2013) introduced the informal stratigraphic unit ‘Bowland-Hodder unit’ (BHU) in the
116 Bowland Basin, referring to the seismically defined unit of Fraser et al. (1990). The base of this
117 informal unit broadly equates to the top of the Chadian carbonates identified in the Widmerpool Gulf
118 while the top of the unit corresponds to the base of the sandstone dominated Millstone Grit (Figure 3).
119 Because of the progradational nature of the Millstone Grit, the top of the Bowland-Hodder is highly
120 diachronous (Aitkenhead et al., 2002; Waters et al., 2007). Andrews (2013) subdivided the BHU into
121 two parts:

- 122 1) a lower unit comprising syn-rift sediments (Chadian–Brigantian) deposited during the
123 formation of the Pennine sub-basins (see above). This unit contains slumps, debri-flows and
124 turbidites and laterally passes to limestone deposited over the highs (Gawthorpe and
125 Clemmey, 1985; Riley, 1990).
- 126 2) an upper unit composed of post-rift sequences (latest Brigantian–Pendleian, locally
127 Arnsbergian, proving its highly diachronous nature) deposited during the period of thermal
128 sag and periodic transgression of an epicontinental sea in combination with deltaic sequences
129 that became more important (Fraser et al., 1990). This unit was informally termed the ‘upper
130 Bowland Shale’ (see also Aitkenhead et al., 2002).

131 The boundary between these two parts has been taken as the onset mudrocks with a characteristic high
132 gamma response on downhole geophysical logs, which has been equated to the Viséan–Namurian

133 (Brigantian–Pendleian) boundary and in terms of biostratigraphy generally coincides with the
134 *Emstites leion* marine band (Andrews, 2013).

135 2.3 The Rempstone 1 and Old Dalby 1 boreholes

136 The two boreholes discussed by Kenomere and co-authors are Rempstone 1 (national grid reference
137 SK 58212 24053; BGS reference number SK52SEBJ39) and Old Dalby 1 (national grid reference
138 SK68143 23703; BGS reference number SK62SEBJ14), both located in the most southern part of the
139 Widmerpool Gulf, close to the northern margin of the Wales-Brabant High (Figure 1). The schematic
140 lithological logs of Yeadonian and older deposits in the boreholes are depicted in Figure 3c following
141 Andrews (2013) and Pharaoh et al. (2011). These logs have been coloured to reflect the lithology in
142 function of the informal BHU introduced in section 2.2 and indicated the intervals for which
143 Kenomere et al. (2017) applied the $\Delta\text{Log R}$ method (black) and the intervals for which Rock-Eval
144 data was published by Andrews (2013). Analysis of Figure 1 and Figure 3 raises two issues:

145 1. Rempstone 1 and Old Dalby 1 are located in the southernmost part of the Widmerpool Gulf, which
146 makes them unrepresentative for the basin as a whole as they are subject to proximal deposition with a
147 high proportion of siliciclastic input. This is reflected in the lithostratigraphic successions (Figure 3):
148 the Bowland Shale Formation laterally passes into the Morridge Formation, it is expected to find
149 thicker deposits of Bowland Shale in the centre and more to the north of the Widmerpool Gulf
150 (Section 2.1). This is apparent in the Duffield 1 core (national grid reference SK 34280 42170, BGS
151 reference number SK34SWBJ5, Aitkenhead, 1977) where a greater proportion of shale is proven than
152 in either Rempstone 1 and Old Dalby 1 (Figure 3).

153 2. Kenomere et al. derive TOC values for the Upper Bowland Shale using the $\Delta\text{Log R}$ technique, and
154 restrict themselves to the Bowland Shale Formation. They then compare the obtained results to the
155 Rock-Eval results published in Andrews (2013) to conclude their measurements are comparable to the
156 pyrolysis results. However, it is important to note that in Rempstone 1 the Rock-Eval results originate
157 from samples from the upper part of the Morridge Formation and in Old Dalby pyrolysis was
158 performed on samples from the Widmerpool Formation. These two formations are very different from
159 the Bowland Shale Formation (see Section 2.1), and therefore a direct comparison is invalid and is a
160 cause of confusion.

161 3. The $\Delta\text{Log R}$ (Passey) methodology

162 To evaluate the conclusions of the Kenomere et al. (2017) study, we applied the $\Delta\text{Log R}$ methodology
163 to the same wireline data used by these authors. The TOC was calculated using the $\Delta\text{Log R}$ method
164 inbuilt into the Senergy Software Interactive Petrophysics™ TOC calculator. The methodology
165 employed in the current paper follows the general method outlined by Gent et al. (2014) in their TOC
166 calculation in the Jurassic shales of the Weald Basin. In the $\Delta\text{Log R}$ method, scaled sonic and

167 resistivity curves overlay in a ‘lean shale’ defined as a non-source shale. When overlain correctly, the
168 TOC curve was well calibrated with the measured TOC from Andrews (2013). As highlighted by
169 Kenomore et al. (2017), the lean shale point is difficult to establish when just considering two wells
170 with limited core data. For this study the lean shale point was chosen to fall in the central part of the
171 Morridge Formation for both Old Dalby 1 and Rempstone 1 (~1250 m and ~690 m respectively).

172 The density and neutron overlay plots were used to verify those of the sonic log. Sonic slowness is
173 preferentially used as it is least susceptible to inaccuracies arising from poor borehole conditions often
174 encountered when drilling shales.

175 A key parameter in the Passey equation for calculating TOC is the level of maturity (LOM), originally
176 derived to calculate coal rank (Passey et al., 1990). The LOM can be calculated from vitrinite
177 reflectance values (Ro) (Hood et al., 1975) (Equation 1; obtained from Schlumberger’s Techlog™
178 software):

$$179 \quad LOM = 0.0989 \times Ro^5 - 2.1587 \times Ro^4 + 12.392 \times Ro^3 - 29.032 \times Ro^2 + 32.53 \times Ro - 3.0338 \quad (1)$$

180 The output TOC curves were calculated first using the expected maturity. The maturity parameters
181 were then adjusted according to variations in the Rock-Eval and vitrinite reflectance data to the
182 maximum and minimum values (Table 3). Shading on the TOC curve in the graphical log plots
183 displays this uncertainty (shading in Figures 4 and 5), where higher maturity values give lower TOC
184 values for a given set of logs and vice versa.

185 Reservoir intervals have to be removed from the calculated TOC curve as the Passey method only
186 accounts for source rocks. This was achieved by applying a volume of clay (VCl) discriminator based
187 on the gamma ray response. Over the Bowland Shale this has no effect as it is in its entirety
188 considered as a shale for the purposes of this calculation. In the overlying Morridge Formation and
189 underlying Widmerpool Formation the shales are interbedded with significant thicknesses of
190 limestone and sandstone, which have been removed, leaving null values in the calculated TOC curve
191 (Figure 4).

192 The vertical resolution of the calculated TOC is limited by the resolution of the logging tools.
193 Therefore, for example, sharply varying TOC values across thinly interbedded shale, coal and sand
194 intervals may be indistinguishable and is likely to be presented as a smoother TOC curve response
195 (Passey et al, 2010). By contrast, each TOC measurement from core or cutting samples represent a
196 single point in the succession.

197 In addition to these points, it is important to highlight the influence of pyrite on petrophysical logs,
198 discussed by amongst others Clavier et al. (1976) and Kennedy (2004). Kenomore and co-authors (p.
199 140) suggest only a completely pyritised section (with a density of 5 g/cm³) will influence
200 measurements and because none of the cores reach that density they conclude pyrite content is

201 negligible. We contest this and in the Morridge Formation pyrite content is so abundant (up to 7.6%;
202 in Carsington Dam Reconstruction Borehole C3, Hennissen et al., 2017) to the point where it
203 influences vitrinite reflectance analysis (Paul C. Hackley, written communication, 2017). For the
204 Bowland Shale Formation similar values (up to 6.7 wt%; Hennissen et al., 2017) have been recorded
205 from the Edale Basin. These values exceed the 5 wt% threshold where a steep decline in resistivity
206 due to pyrite influence has been reported (Clavier et al., 1976; Clennell et al., 2010) and therefore it
207 can be expected that the results of the Passey method as applied by Kenomore and co-authors will
208 have been influenced by the pyrite presence.

209 4. The $\Delta\text{Log R}$ method on Rempstone 1 and Old Dalby 1

210 The methodology detailed in Section 3 was applied to the geophysical logs of Rempstone 1 and Old
211 Dalby 1 to produce Figure 4. To calibrate the TOC calculations, we use vitrinite reflectance data from
212 Coombes et al. (1986) in Rempstone 1 (Table 1) and T_{max} calculated Ro data from Andrews (2013) in
213 both boreholes (Table 2) to determine the LOM presented in Table 3. Also included in Figure 4 are
214 the results presented by Kenomore and co-authors.

215 Analysis of Figure 4 clearly shows:

- 216 1. Kenomore et al. (2017) calibrated Rempstone 1 and Old Dalby 1 TOC outputs with
217 calculated maturity values from intervals outside the stratigraphic limits of the Bowland
218 Shale Formation. In the Rempstone 1 Borehole they used a fixed average calculated Ro of
219 0.71 (T_{max} of 437°C) based on the 5 measurements from Andrews (2013) in the
220 Morridge Formation (Table 1) while in Old Dalby 1 these authors used the lower estimate
221 of 0.6 for Ro.
- 222 2. In Figure 4a, we present a curve calibrated using additional vitrinite reflectance
223 measurements from the end of well report from Rempstone 1 (Coombes et al., 1986).
224 These measured vitrinite reflectance values are taken to be more reliable than the T_{max}
225 equivalent Ro (T_{max} eq. Ro) from Andrews (2013) as they are a direct measurement: T_{max}
226 eq. Ro is acquired using the Jarvie et al. (2001) equation, calibrated for the Barnett Shale,
227 which may introduce errors when used in a different setting (e.g. Wüst et al. 2013). Here,
228 we find an increase in TOC with larger uncertainties, especially in the Bowland Shale
229 Formation (purple curve, Figure 4a). However, the results from Kenomore et al. (2017)
230 seem to correlate better with this calculated curve rather than the Rock-Eval calculated
231 values from Andrews (2013) (blue curve in Figure 4a).
- 232 3. Calibration of the calculated TOC curves in Old Dalby 1 is very difficult. The
233 interbedded nature of the Widmerpool Formation (the source of the Rock-Eval data) do
234 not represent a thick shale sequence preferred when calibrating the calculations.

235 These three points show the influence of the original Rock-Eval data on the outcome of the calculated
236 TOC. None of these measurements from Andrews (2013) were performed on the interval targeted by
237 Kenomore et al. (2017). Given the highly interbedded nature and sedimentologically diverse character
238 of both the Widmerpool Formation and the Morridge Formation (Section 2), where the Rock-Eval
239 measurements were made, it is unlikely these represent the same depositional environments reflected
240 by the Bowland Shale Formation. Therefore, we believe that the statement by Kenomore et al. (2017)
241 that the results of the study correlate well with the average values of previously published BGS data is
242 misleading. Moreover, it is important to note that the Passey method was intended for identifying and
243 calculating TOC in organic-rich rocks (Passey et al., 1990), but not for resource play evaluation (see
244 also Lecompte and Hursan, 2010).

245 5. Conclusions

246 In reviewing the study published by Kenomore et al. (2017) we uncovered several flaws which mostly
247 reflect poor consideration of the geological setting of the Carboniferous deposits in the Widmerpool
248 Gulf. These can be subdivided into geological and methodological concerns:

249 Geological concerns:

- 250 1) The thermal maturity utilised to calibrate the TOC calculations in the Passey methodology for
251 the Bowland Shale Formation were from different formations. In the Rempstone 1 Borehole,
252 Rock-Eval measurements from the Morridge Formation while in Old Dalby 1 Rock-Eval
253 measurements from the Widmerpool Formation were used.
- 254 2) Both wells investigated by Kenomore and co-authors were located in the southernmost part of
255 the Widmerpool Gulf. Only a very thin interval of Bowland Shale was proven in these
256 boreholes making them unsuitable datapoints representing of the Widmerpool Gulf as a
257 whole.
- 258 3) Pyrite is a major component in the Carboniferous mudstones of the Widmerpool Gulf
259 surpassing the 5 wt.% threshold where it has shown to have an influence on the well log
260 responses.

261 Methodological concerns:

- 262 1) The Rock-Eval data used for the calibration of the maturity comes from interbedded
263 formations and no information of the lithology of these samples is known; the Morridge and
264 Widmerpool formations are heterolithic mudstone-sandstone successions. The provenance of
265 the organic material and the TOC as a whole in the mudstones and sandstones is different and
266 these changes occur at a higher resolution than the resolution of the geophysical logs.

267 2) No robust geochemical data set is available to calibrate the calculation.

268 We recommend that more geochemical data is collected to calibrate the TOC models and that this
269 occurs in the formations that are the subject of the modelling exercise. This should then be repeated
270 for more wells and over a larger area within the Widmerpool Gulf, in order to make the extrapolations
271 credible. It is important to realise the limitations of the $\Delta\text{Log R}$ methodology. We believe the $\Delta\text{Log R}$
272 method could be used as a steering tool to identify intervals of interest but because of the
273 heterogeneous nature of the Carboniferous deposits it falls short to perform a meaningful assessment
274 of the potential resource and more traditional multi-proxy approaches need to be applied (e.g. Rock-
275 Eval, palynofacies analysis, X-ray diffraction and carbon isotope analysis). This is mostly due to the
276 onus being placed on the level of maturity (LOM) in its derivation. Because of the variable lithology
277 and with it, variable organic content and character, we believe the $\Delta\text{Log R}$ methodology is not a
278 viable replacement for traditional TOC determinations (eg. Rock-Eval pyrolysis) in the Widmerpool
279 Gulf.

280 Acknowledgements

281 Both authors publish with the approval of the Executive Director of The British Geological Survey.
282 Ed Hough is thanked for comments and suggestions on an earlier draft of this manuscript.

283 Figure Captions

284 Figure 1: Mississippian paleogeography of the UK (A) and a focus on the Widmerpool Gulf and
285 adjacent areas with the boreholes discussed in the text.

286 Figure 2: Stratigraphic column in the Bowland Basin, Edale Basin and Widmerpool Gulf plotted, with
287 the Bowland Shale Formation highlighted, against the local (Holliday and Molyneux, 2006) and
288 global (Davydov et al., 2012) chronostratigraphy (modified after Hennissen et al., 2017).

289 Figure 3: The informal Bowland-Hodder Unit (BHU); A: Schematic diagram of the BHU in a fault-
290 bounded sub basin of the Pennine basin (modified after Andrews, 2013); B: idealized succession
291 through the Millstone Grit and Bowland Hodder unit (modified after Andrews, 2013); C: schematic
292 logs of four key Widmerpool boreholes, Duffield (following Gross et al., 2014), Carsington Dam
293 composite (following Aitkenhead, 1991; Aitkenhead et al., 2002), Rempstone 1 (following Pharaoh et
294 al., 2011) and Old Dalby 1 (following Pharaoh et al., 2011).

295 Figure 4: Comparison of the $\Delta\text{Log R}$ methodology applied to the Rempstone 1 borehole. Note the
296 position of the cored intervals which form the bases of the Rock Eval analysis presented in Andrews
297 (2013). Shaded envelopes in curves 5a and 5b represent uncertainty intervals for the calculated TOC.

298 Figure 5: Comparison of the $\Delta\text{Log R}$ methodology applied to the Old Dalby 1 borehole. Note the
299 position of the cored intervals which form the bases of the Rock Eval analysis presented in Andrews
300 (2013). Shaded envelopes in curves 5a and 5b represent uncertainty intervals for the calculated TOC.

301 Figure 6: A crossplot of TOC and S₂, indicative of hydrocarbons formed during thermal
302 decomposition, in Widmerpool Gulf samples. Data from Hennissen et al. (2017) and Andrews (2013).

303 References

304 Aitkenhead, N., 1977. The Institute of Geological Sciences Borehole at Duffield, Derbyshire. Bull.
305 Geol. Surv. G. B. 59, pp. 60.

306 Aitkenhead, N., 1991. Carsington Dam Reconstruction: notes on the stratigraphy and correlation of
307 groundwater monitoring, BGS Tech. Rep. British Geological Survey, Keyworth, Nottingham (U.K.),
308 pp. 22.

309 Aitkenhead, N., Barclay, W.J., Brandon, A., Chadwick, R., Chisholm, J.I., Cooper, A.H., Johnson,
310 E.W., 2002. British Regional Geology: the Pennines and Adjacent Areas. British Geological Survey,
311 Nottingham, UK, pp. 206.

312 Aitkenhead, N., Chisholm, J.I., 1982. A standard nomenclature for the Dinantian formations of the
313 Peak District of Derbyshire and Staffordshire. Inst. Geol. Sci. Rep. 82/8, H.M.S.O., London, pp. 24.

314 Andrews, I.J., 2013. The Carboniferous Bowland Shale Gas Study: Geology and Resource
315 Estimation. British Geological Survey for the Department of Energy and Climate Change, London,
316 UK, 64 pp.
317 [https://www.gov.uk/government/uploads/system/uploads/attachment_data/file/226874/BGS_DECC_](https://www.gov.uk/government/uploads/system/uploads/attachment_data/file/226874/BGS_DECC_BowlandShaleGasReport_MAIN_REPORT.pdf)
318 [BowlandShaleGasReport_MAIN_REPORT.pdf](https://www.gov.uk/government/uploads/system/uploads/attachment_data/file/226874/BGS_DECC_BowlandShaleGasReport_MAIN_REPORT.pdf)

319 Bisat, W.S., 1923. The Carboniferous Goniaticites of the North of England and their Zones. Proc.
320 Yorkshire Geol. Soc. 20, 40–124. <http://dx.doi.org/10.1144/pygs.20.1.40>.

321 Clavier, C., Heim, A., Scala, C., 1976. Effect Of Pyrite On Resistivity And Other Logging
322 Measurements, SPWLA 17th Annual Logging Symposium. Society of Petrophysicists and Well-Log
323 Analysts, Denver, Colorado.

324 Clennell, M.B., Josh, M., Esteban, L., Piane, C.D., Schmid, S., Verrall, M., Hill, D., Woods, C.,
325 McMullan, B., 2010. The Influence Of Pyrite On Rock Electrical Properties: A Case Study From Nw
326 Australian Gas Reservoirs, SPWLA 51st Annual Logging Symposium. Society of Petrophysicists and
327 Well-Log Analysts, Perth, Australia.

328 Coombes, D., Hughes, J., Maile, C.N., Batten, D.J., 1986. A Geochemical Evaluation of Sediment and
329 Oil Samples from the Well Rempstone-1, East Midlands, UK Land. BP Research Centre, Sunbury-on-
330 Thames, pp. 54.

331 Davies, J.R., Wilson, D., Williamson, I.T., 2004. Geology of the country around Flint, Mem. BGS.
332 British Geological Survey, Keyworth, Nottingham, pp. 212.

333 Davydov, V.I., Korn, D., Schmitz, M.D., Gradstein, F.M., Hammer, O., 2012. Chapter 23 - The
334 Carboniferous Period, in: Gradstein, F.M., Ogg, J.G., Schmitz, M.D., Ogg, G.M. (Eds.), The Geologic
335 Time Scale. Elsevier, Boston, pp. 603–651. <http://dx.doi.org/10.1016/B978-0-444-59425-9.00023-8>.

- 336 Fraser, A.J., Nash, D.F., Steele, R.P., Ebdon, C.C., 1990. A regional assessment of the intra-
337 Carboniferous play of Northern England. *Geol. Soc., London, Spec. Pub.* 50, 417–440.
338 <http://dx.doi.org/10.1144/gsl.sp.1990.050.01.26>.
- 339 Gawthorpe, R.L., 1987. Tectono-sedimentary evolution of the Bowland Basin, N England, during the
340 Dinantian. *J. Geol. Soc.* 144, 59–71. <http://dx.doi.org/10.1144/gsjgs.144.1.0059>.
- 341 Gawthorpe, R.L., Clemmey, H., 1985. Geometry of submarine slides in the Bowland Basin
342 (Dinantian) and their relation to debris flows. *J. Geol. Soc.* 142, 555-565.
343 <http://dx.doi.org/10.1144/gsjgs.142.3.0555>.
- 344 Gent, C.M.A., Hannis, S.D., Andrews, I.J., 2014. Appendix D: Estimation of total organic carbon in
345 the Jurassic shales of the Weald area by log analysis, *in: The Jurassic shales of the Weald Basin: geology and shale oil and shale gas resource estimation* (ed. Andrews, I. J.). British Geological
346 Survey for the Department of Energy and Climate Change, London, UK, 76 pp.
347
- 348 Gross, D., Sachsenhofer, R.F., Bechtel, A., Pytlak, L., Rupprecht, B., Wegerer, E., 2014. Organic
349 geochemistry of Mississippian shales (Bowland Shale Formation) in central Britain: Implications for
350 depositional environment, source rock and gas shale potential. *Mar. Pet. Geol.* 59, 1–21.
351 <http://dx.doi.org/10.1016/j.marpetgeo.2014.07.022>.
- 352 Hennissen, J.A.I., Hough, E., Vane, C.H., Leng, M.J., Kemp, S.J., Stephenson, M.H., 2017. The
353 prospectivity of a potential shale gas play: An example from the southern Pennine Basin (central
354 England, UK). *Mar. Pet. Geol.* 86, 1047–1066. <http://dx.doi.org/10.1016/j.marpetgeo.2017.06.033>.
- 355 Holdsworth, B.K., Collinson, J.D., 1988. Millstone Grit cyclicity revisited, *in: Besly, B.M., Kelling, G. (Eds.), Sedimentation in a synorogenic basin complex.* Blackie, Glasgow, UK, pp. 132–152.
356
- 357 Holliday, D.W., Molyneux, S.G., 2006. Editorial statement: new official names for the subsystems,
358 series and stages of the Carboniferous System – some guidance for contributors to the *Proceedings*.
359 *Proc. Yorkshire Geol. Soc.* 56, 57–58. <http://dx.doi.org/10.1144/pygs.56.1.57>.
- 360 Hood, A., Gutjahr, C.C.M., Heacock, R.L., 1975. Organic metamorphism and the generation of
361 petroleum. *AAPG Bull.* 59, 986–996.
- 362 Isbell, J.L., Miller, M.F., Wolfe, K.L., Lenaker, P.A., 2003. Timing of Paleozoic glaciation in
363 Gondwana: was glaciation responsible for the development of Northern Hemisphere cyclothem?, *in:*
364 Chan, M.A., Archer, A.W. (Eds.), *Extreme Depositional Environments: Mega End Members in*
365 *Geologic Time.* Geological Society of America, Special Papers, Boulder, Colorado, pp. 5–24.
- 366 Jarvie, D.M., Claxton, B.L., Henk, F., Breyer, J.T., 2001. Oil and Shale Gas from the Barnett Shale,
367 Ft. Worth Basin, Texas, AAPG Annual Convention. AAPG, Denver, CO, pp. 28.
- 368 Kennedy, M.C., 2004. Gold Fool's: Detecting, Quantifying And Accounting For The Effects Of Pyrite
369 On Modern Logs, SPWLA 45th Annual Logging Symposium. Society of Petrophysicists and Well-
370 Log Analysts, Noordwijk, Netherlands.
- 371 Kenomore, M., Hassan, M., Dhakal, H., Shah, A., 2017. Total organic carbon evaluation of the
372 Bowland Shale Formation in the Upper Bowland of the Widmerpool Gulf. *J. Pet. Sci. Eng.* 150, 137-
373 145 <http://doi.org/10.1016/j.petrol.2016.11.040>.
- 374 Lecompte, B., Hursan, G., 2010. Quantifying Source Rock Maturity From Logs: How To Get More
375 Than TOC From Delta Log R, SPE Annual Technical Conference and Exhibition. Soc. Pet. Eng.,
376 Florence, Italy. <http://dx.doi.org/10.2118/133128-MS>.

- 377 Leeder, M.R., 1982. Upper Palaeozoic basins of the British Isles—Caledonide inheritance versus
378 Hercynian plate margin processes. *J. Geol. Soc.* 139, 479–491.
379 <http://dx.doi.org/10.1144/gsjgs.139.4.0479>.
- 380 Leeder, M.R., McMahon, A.H., 1988. Tests and consequences of the extensional theory for
381 Carboniferous basin evolution in Northern England, in: Besly, B.M., Kelling, G. (Eds.),
382 Sedimentation in a Synorogenic Basin Complex: the Upper Carboniferous of Northwest Europe.
383 Blackie, Glasgow and London, pp. 43–52.
- 384 Martinsen, O.J., Collinson, J.D., Holdsworth, B.K., 1995. Millstone Grit Cyclicity Revisited, II:
385 Sequence Stratigraphy and Sedimentary Responses to Changes of Relative Sea-Level, Sedimentary
386 Facies Analysis. Blackwell Publishing Ltd., pp. 305–327
387 <http://dx.doi.org/10.1002/9781444304091.ch13>.
- 388 Passey, Q.R., Creaney, S., Kulla, J.B., Moretti, F.J., Stroud, J.D., 1990. A practical model for organic
389 richness from porosity and resistivity logs. *AAPG Bull.* 74, 1777–1794.
- 390 Pharaoh, T.C., Vincent, C., Bentham, M.S., Hulbert, A.G., Waters, C.N., Smith, N.J.P., 2011.
391 Structure and evolution of the East Midlands region of the Pennine Basin, *Subsurf. Mem. BGS.*
392 British Geological Survey, Keyworth, UK, pp. 156.
- 393 Ramsbottom, W.H.C., 1977. Major Cycles of Transgression and Regression (Mesothems) in the
394 Namurian. *Proc. Yorkshire Geol. Soc.* 41, 261–291. <http://dx.doi.org/10.1144/pygs.41.3.261>.
- 395 Ramsbottom, W.H.C., Rhys, G.H., Smith, E.G., Bullerwell, W., Cosgrove, M.E., Elliot, R.W., 1962.
396 Boreholes in the Carboniferous rocks of the Ashover district, Derbyshire. *Bull. Geol. Surv. G. B.* 19,
397 75–168.
- 398 Riley, N.J., 1990. Stratigraphy of the Worston Shale Group (Dinantian), Craven Basin, north-west
399 England. *Proc. Yorkshire Geol. Soc.* 48, 163–187.
- 400 Selley, R.C., 1987. British shale gas potential scrutinized. *Oil Gas J.* 15, 62–64.
- 401 Smith, N., Turner, P., Williams, G., 2010. UK data and analysis for shale gas prospectivity. *Petroleum*
402 *Geology Conference Series* 7, 1087–1098.
- 403 Stephenson, M.H., Millward, D., Leng, M.J., Vane, C.H., 2008. Palaeoecological and possible
404 evolutionary effects of early Namurian (Serpukhovian, Carboniferous) glacioeustatic cyclicity. *J.*
405 *Geol. Soc.* 165, 993–1005 <http://dx.doi.org/10.1144/0016-76492007-153>.
- 406 Veevers, J.J., Powell, C.M., 1987. Late Paleozoic glacial episodes in Gondwanaland reflected in
407 transgressive-regressive depositional sequences in Euramerica. *GSA Bull.* 98, 475–487.
408 [http://dx.doi.org/10.1130/0016-7606\(1987\)98<475:LPGEIG>2.0.CO;2](http://dx.doi.org/10.1130/0016-7606(1987)98<475:LPGEIG>2.0.CO;2).
- 409 Waters, C.N., Browne, M.A.E., Dean, M.T., Powell, J.H., 2007. Lithostratigraphical framework for
410 Carboniferous successions of Great Britain (Onshore). *Res. Rep. 07/01.* British Geological Survey,
411 Keyworth, Nottingham, UK, pp. 70.
- 412 Waters, C.N., Condon, D.J., 2012. Nature and timing of Late Mississippian to Mid-Pennsylvanian
413 glacio-eustatic sea-level changes of the Pennine Basin, UK. *J. Geol. Soc.* 169, 37–51.
414 <http://dx.doi.org/10.1144/0016-76492011-047>.
- 415 Waters, C.N., Waters, R.A., Barclay, W.J., Davies, J.R., 2009. A lithostratigraphical framework for
416 the Carboniferous successions of southern Great Britain (onshore), *Res. Rep. 09/01.* British
417 Geological Survey, Keyworth, Nottingham, UK, pp. 194.

418 Wüst, R.A.J., Hackley, P., Nassichuk, B.R., 2013. Vitrinite reflectance versus pyrolysis Tmax data:
419 Assessing thermal maturity in shale plays with special reference to the Duvernay shale play of the
420 Western Canadian Sedimentary Basin, Alberta, Canada. SPE International, SPE 167031.

421

422 **Figure Captions**

423 Figure 1: Mississippian paleogeography of the UK (A) and a focus on the Widmerpool Gulf and
424 adjacent areas with the boreholes discussed in the text.

425 Figure 2: Stratigraphic column in the Bowland Basin, Edale Basin and Widmerpool Gulf plotted, with
426 the Bowland Shale Formation highlighted, against the local (Holliday and Molyneux, 2006) and
427 global (Davydov et al., 2012) chronostratigraphy (modified after Hennissen et al., 2017).

428 Figure 3: The informal Bowland-Hodder Unit (BHU); A: Schematic diagram of the BHU in a fault-
429 bounded sub basin of the Pennine basin (modified after Andrews, 2013); B: idealized succession
430 through the Millstone Grit and Bowland Hodder unit (modified after Andrews, 2013); C: schematic
431 logs of four key Widmerpool boreholes, Duffield (following Gross et al., 2014), Carsington Dam
432 composite (following Aitkenhead, 1991; Aitkenhead et al., 2002), Rempstone 1 (following Pharaoh et
433 al., 2011) and Old Dalby 1 (following Pharaoh et al., 2011).

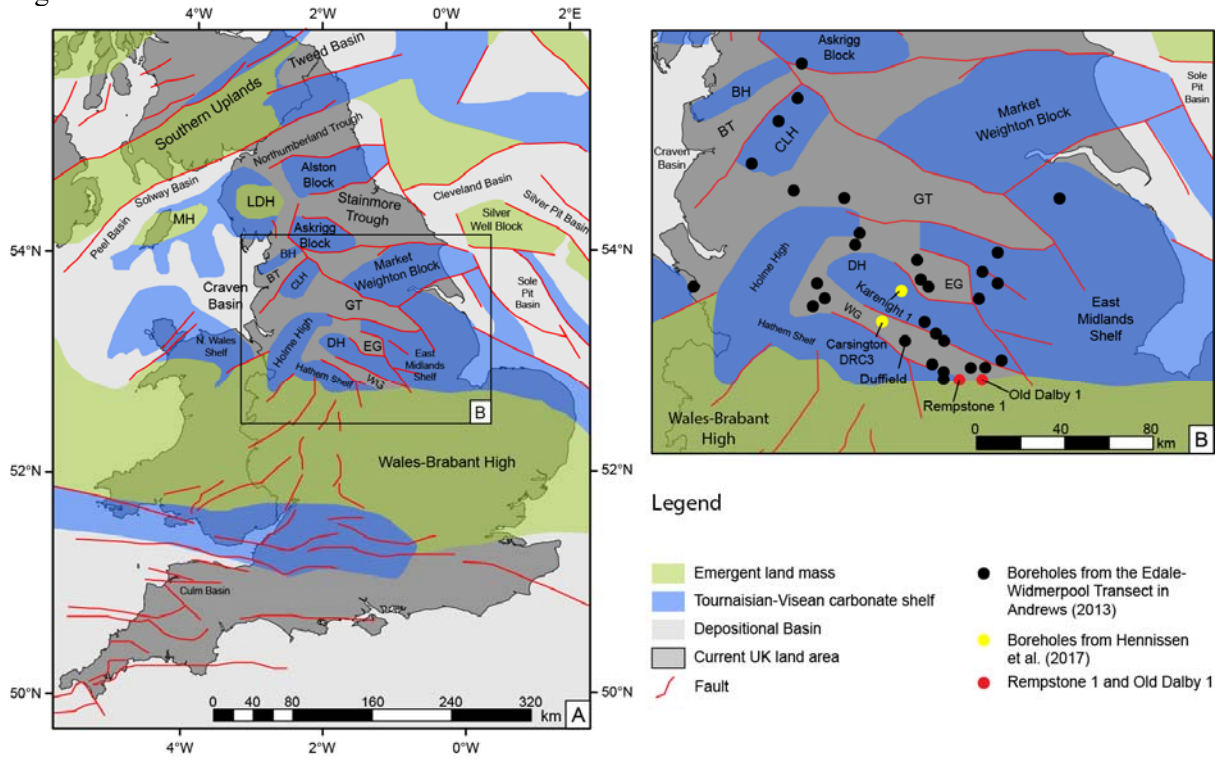
434 Figure 4: Comparison of the $\Delta\text{Log R}$ methodology applied to the Rempstone 1 borehole. Note the
435 position of the cored intervals which form the bases of the Rock Eval analysis presented in Andrews
436 (2013). Shaded envelopes in curves 5a and 5b represent uncertainty intervals for the calculated TOC.

437 Figure 5: Comparison of the $\Delta\text{Log R}$ methodology applied to the Old Dalby 1 borehole. Note the
438 position of the cored intervals which form the bases of the Rock Eval analysis presented in Andrews
439 (2013). Shaded envelopes in curves 5a and 5b represent uncertainty intervals for the calculated TOC.

440 Figure 6: A crossplot of TOC and S₂, indicative of hydrocarbons formed during thermal
441 decomposition, in Widmerpool Gulf samples. Data from Hennissen et al. (2017) and Andrews (2013).

442

443 Figure 1



444

445

446

447

448

449

450

451

452

453

454

455

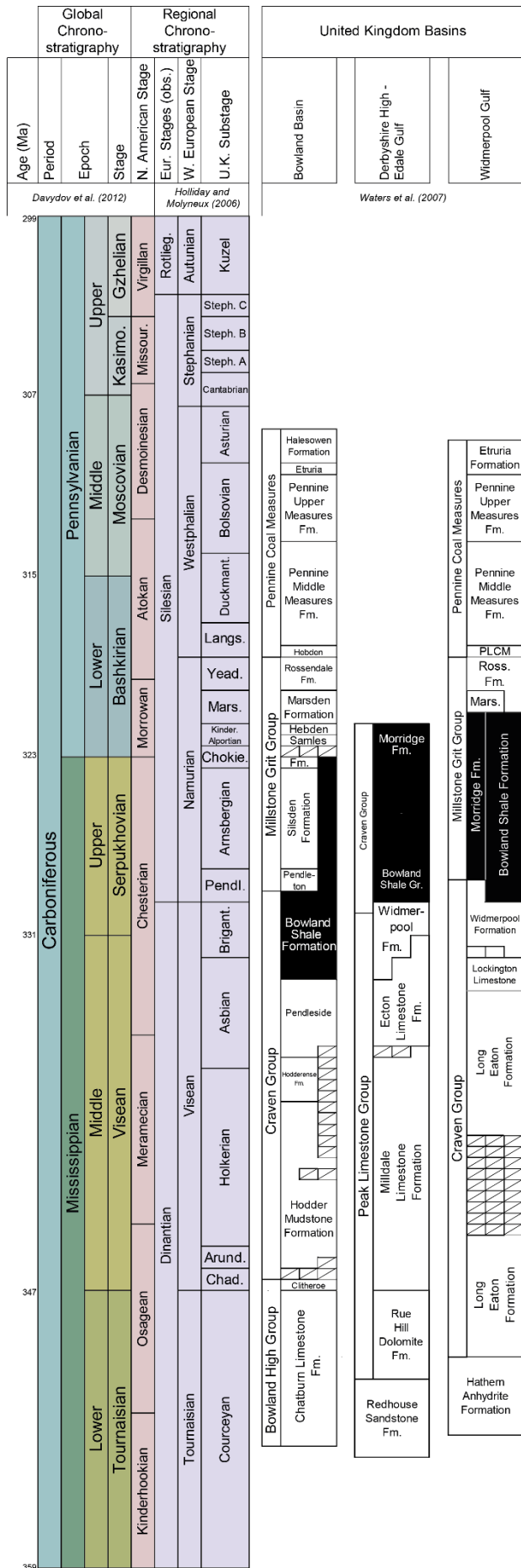
456

457

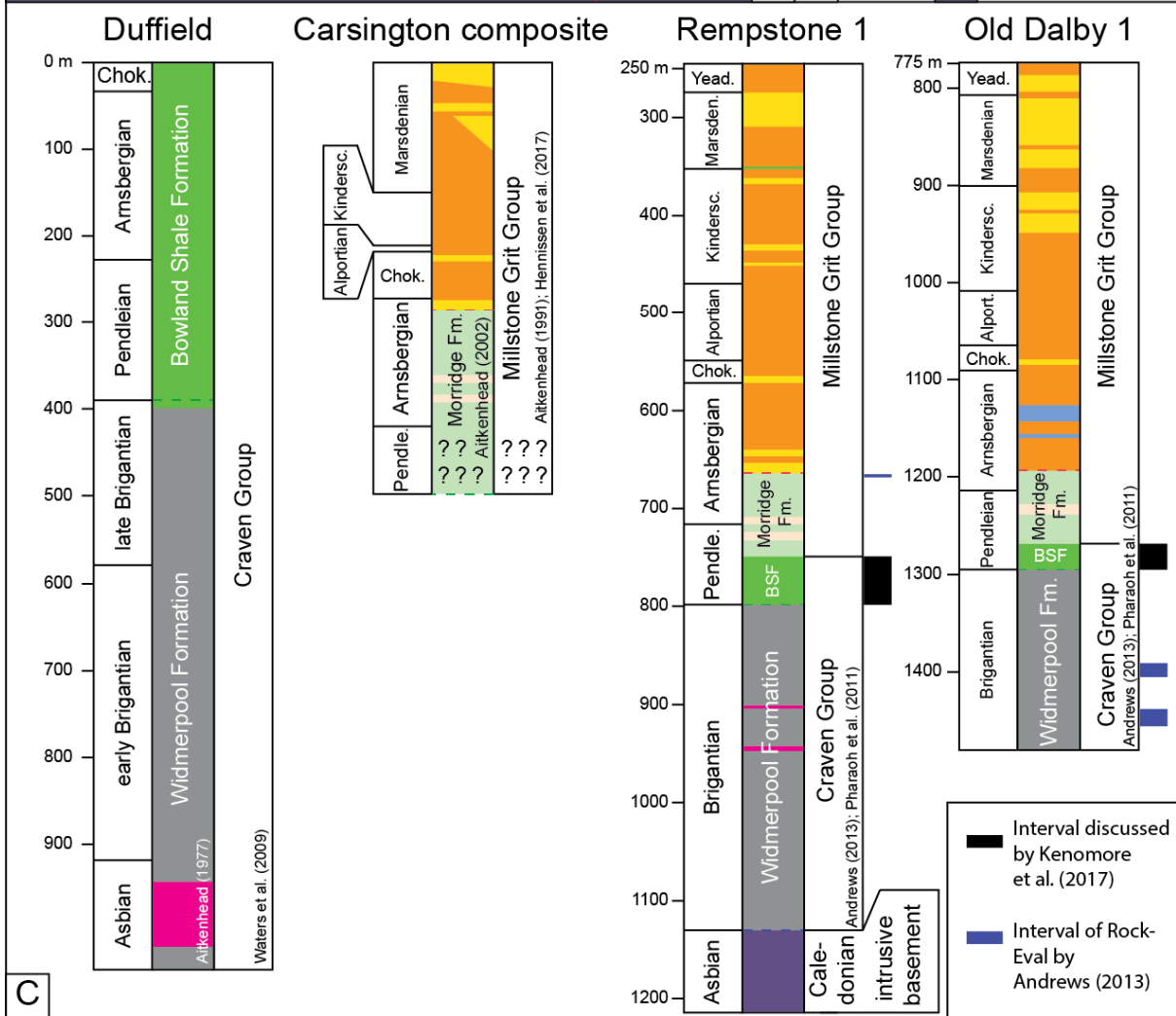
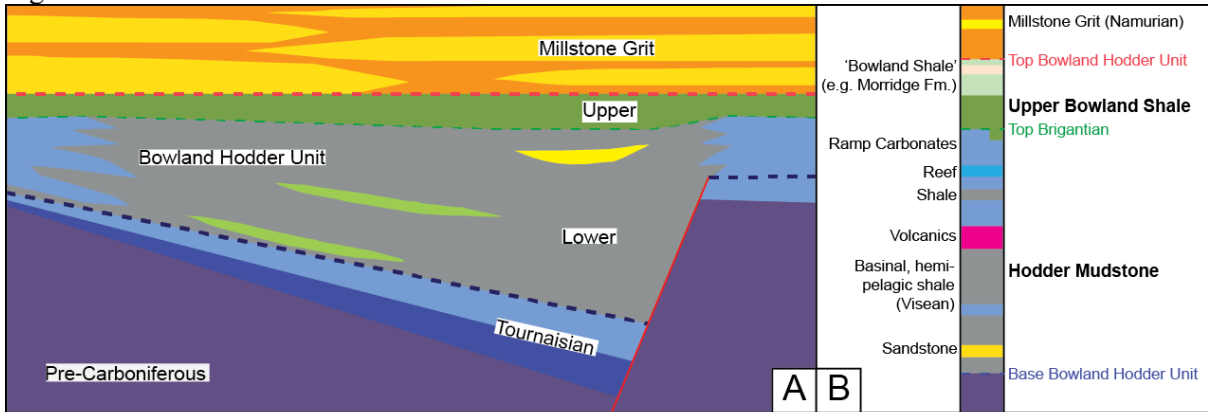
458

459

460 Figure 2 (next page)



462 Figure 3



463

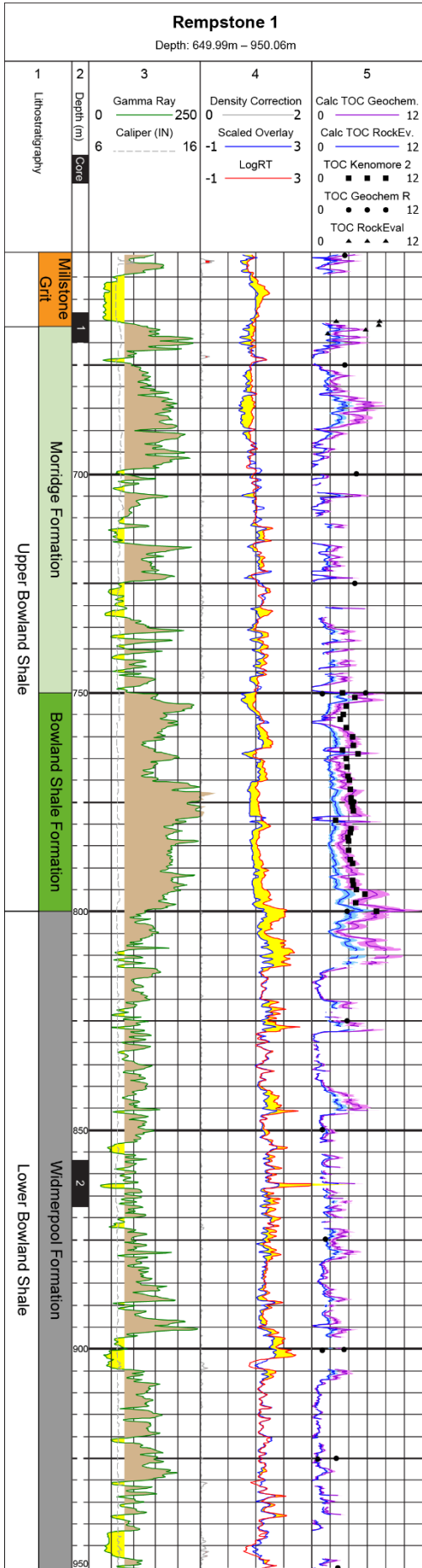
464

465

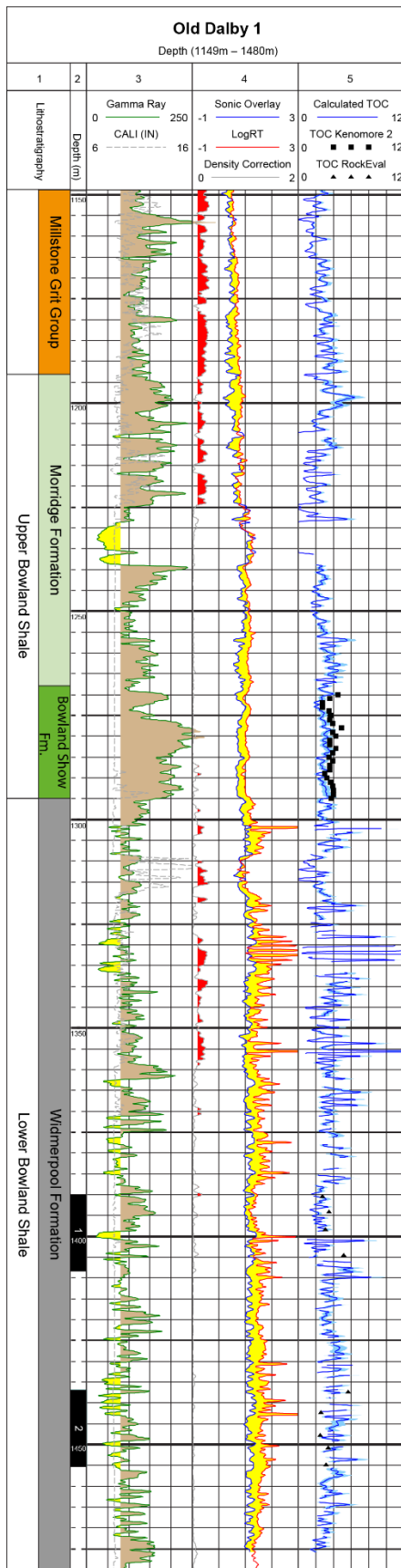
466

467

468 Figure 4 (next page)



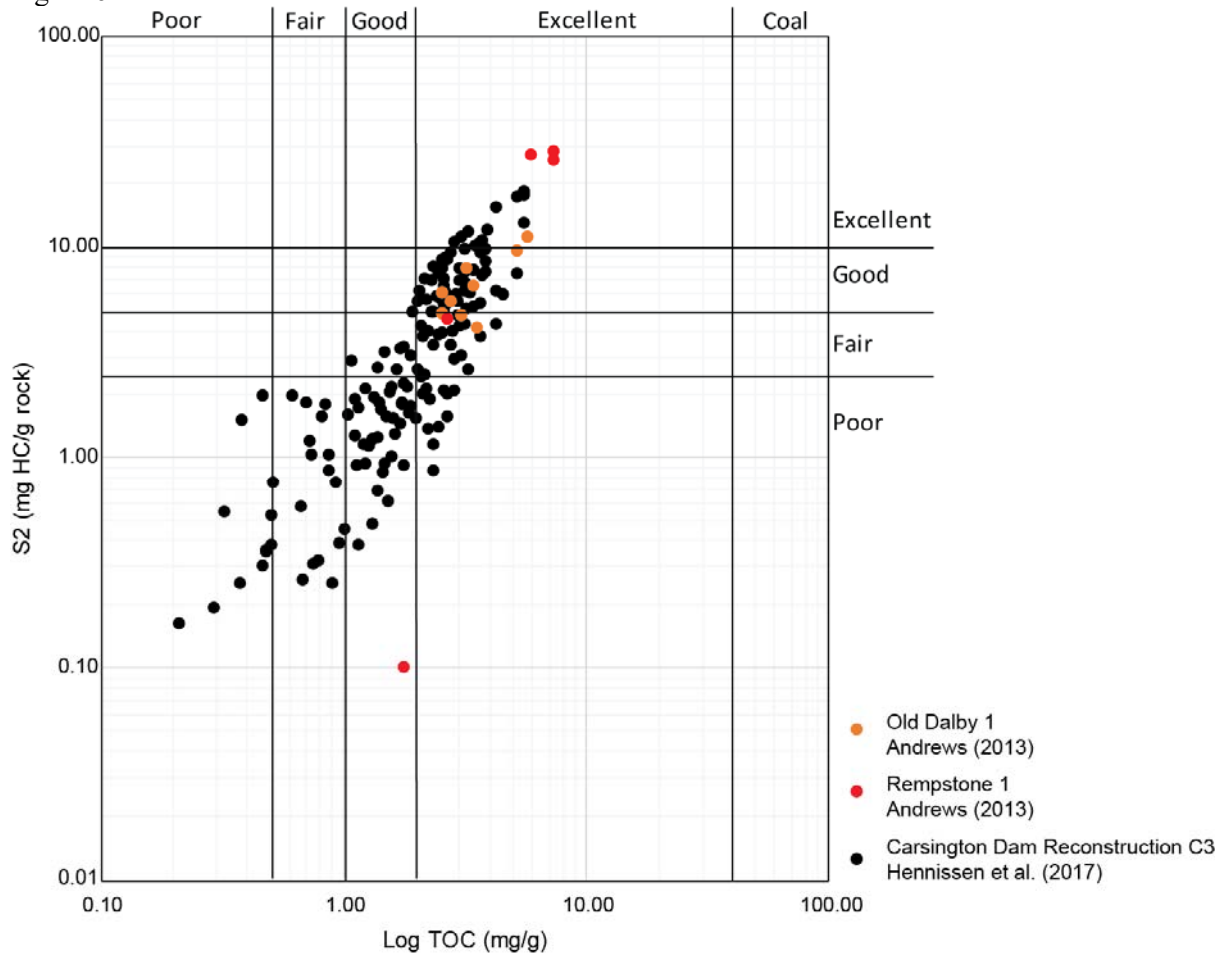
470 Figure 5



471

472

473 Figure 6



474

475

476

477 Tables

478 Tables

479 Table 1: Rock-Eval and vitrinite reflectance results from Coombes et al. (1986) in the Rempstone 1
480 borehole

481

Rempstone 1		
Coombes et al. (1986)		
Depth (m)	TOC (%)	%Ro
650	3.6	0.5
675	3.6	
700	4.8	
725	4.7	
750	5.8	0.5
775	4.6	
800	3.8	
825	3.8	
850	1.2	0.46
875	1.5	
900	3.5	
925	2.7	
950	2.8	0.44

482

483 Table 2: Rock-Eval results from Andrews (2013) in the Old Dalby 1 and Rempstone 1 boreholes

Rempstone 1					Old Dalby 1				
Depth (m)	Depth (ft)	TOC (wt. %)	T _{max} (°C)	T _{max} R _o	Depth (m)	Depth (ft)	TOC (wt.%)	T _{max} (°C)	T _{max} R _o
665.0	2181.8	2.66	437	0.71	1390.6	4562.3	2.73	436	0.69
665.3	2182.7	7.31	437	0.71	1394.3	4574.5	3.53	433	0.63
666.0	2185	7.29	438	0.72	1398.5	4588.3	3.06	434	0.65
667.0	2188.3	5.87	437	0.71	1404.6	4608.3	5.12	432	0.62
668.0	2191.6	1.77	431	0.60	1437.5	4716.2	5.65	435	0.67
					1442.5	4732.6	2.55	434	0.65
					1447.8	4750	2.54	436	0.69
					1450.8	4759.8	3.40	438	0.72
					1455.0	4773.6	3.18	436	0.69
Average:		4.98	436	0.69	Average:		3.53	435	0.67

484

485 Table 3: Level of Organic Maturity (LOM) and equivalent vitrinite reflectance values and sources
486 used in the TOC calculation. The error margins are represented by blue shading on the graphical log
487 plot (Figure 4). *Ro calculated from Tmax using the following equation following Jarvie et al. (2001)
488 $Ro = 0.0189 \times Tmax - 7.16$ Where Tmax is in degrees Celsius.

489

	Bowland Shale & Morridge Formation		Widmerpool Formation	
	Vitrinite Reflectance (Ro)	Level of Maturity (LOM)	Vitrinite Reflectance (Ro)	Level of Maturity (LOM)
Rempstone 1				
Rock-Eval and Ro data (Coombes et al., 1986)	0.51 ±0.04	7.5 ±0.5	0.56 ±0.05	8.0 ±0.5
Rock-Eval data (Andrews, 2013)	0.69 ±0.07*	9.2 ±0.5	0.73 ±0.07*	9.5 ±0.5
Old Dalby 1				
Rock-Eval data* (Andrews, 2013)	0.61 ±0.05*	8.5 ±0.5	0.66 ±0.06*	9.0 ±0.5

490

491